IEEE Photonics Journal
An IEEE Photonics Society Publication

Open Access

High Efficiency 1.9 kW Single Diode Laser Bar Epitaxially Stacked With a Tunnel Junction

Volume 13, Number 3, June 2021

Yuliang Zhao
Zhenfu Wang
Abdullah Demir
Guowen Yang
Shufang Ma
Bingshe Xu
Cheng Sun
Bo Li
Bocang Qiu

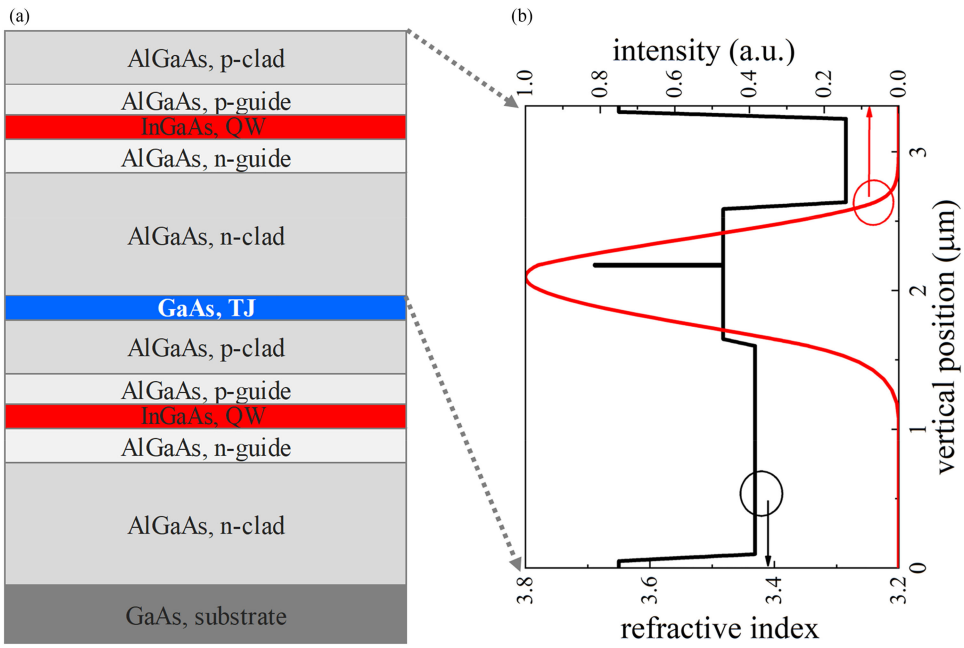

DOI: 10.1109/JPHOT.2021.3073732

High Efficiency 1.9 kW Single Diode Laser Bar Epitaxially Stacked With a Tunnel Junction

Yuliang Zhao [1,2] Zhenfu Wang [1] Abdullah Demir [5] Guowen Yang,[1,2] Shufang Ma [3] Bingshe Xu,[3] Cheng Sun,[4] Bo Li,[4] and Bocang Qiu[1]

[1]State Key Laboratory of Transient Optics and Photonics, Xi'an Institute of Optics and Precision Mechanics, Chinese Academy of Sciences, Xi'an 710119, China
[2]University of Chinese Academy of Sciences, Beijing 100049, China
[3]Institute of Atomic and Molecular Science, Shaanxi University of Science and Technology, Xi'an 710021, China
[4]Lumcore Optoelectronics Tech. Company Ltd., Xi'an 710071, China
[5]Bilkent University, UNAM - Institute of Materials Science and Nanotechnology, Ankara 06800, Turkey

DOI:10.1109/JPHOT.2021.3073732

Manuscript received January 28, 2021; revised March 29, 2021; accepted April 12, 2021. Date of publication April 16, 2021; date of current version May 18, 2021. This work was supported in part by Project of Xi'an Institute of Optics and Precision Mechanics, Chinese Academy of Sciences Y855J61213, in part by National Natural Science Foundation of China under Grant 61504167, and in part by the Natural Science Foundation of Shaanxi Province under Grant 2015JQ6263. Corresponding authors: Zhenfu Wang and Bocang Qiu (e-mail: wzf2718@opt.ac.cn; qiubocang@opt.ac.cn).

Abstract: We report on the development of a 940-nm diode laser bar based on epitaxially stacked active regions by employing a tunnel junction structure. The tunnel junction and the device parameters were systematically optimized to achieve high output and power conversion efficiency. A record quasi-continuous wave (QCW) peak power of 1.91 kW at 25 °C was demonstrated from a 1-cm wide bar with a 2-mm cavity length at 1 kA drive current (200 μs pulse width and 10 Hz repetition rate). Below the onset of the thermal rollover, the slope efficiency was as high as 2.23 W/A. The maximum power conversion efficiency of 61.1% at 25 °C was measured at 300 A. Reducing the heatsink temperature to 15 °C led to a marginal increase in the peak power to 1.95 kW.

Index Terms: Semiconductor laser, diode laser bar, high power, power conversion efficiency, tunnel junction.

1. INTRODUCTION

High power diode lasers based on GaAs material system have found a variety of applications such as solid-state laser and fiber laser pumping because of their excellent performance in power level, power conversion efficiency (PCE), and reliability [1], [2]. Diode laser bars are the most effective sources for end or side pumping of bulk solid-state lasers, where a 1-cm wide bar or its stacks are a common configuration [2]–[10]. In these applications, diode laser pumps usually operate in two different modes, the continuous-wave (CW) mode with power levels ranging from tens to hundreds of watts or the quasi-continuous wave (QCW) mode with increased power levels to kilowatts. Since the pump laser operates with a sufficiently short pulse width and low duty cycle in QCW mode [3], much higher peak power can be obtained without degrading power conversion efficiency and

reliability due to the significant suppression of the self-heating effect. Increasing the output power, efficiency, and brightness of bars would directly improve the performance and reduce the cost of these systems; hence, an efficient increase of output power is a high priority.

Early in 2004, Li *et al.* reported 940-nm CW optical power of 210 W for a 1-cm laser bar with 1.3 mm cavity length and 37% bar fill factor (here the fill factor (FF) is defined as the ratio of the injected area to the total bar area) [4]. In 2007, Jenoptik demonstrated the first 1 kW output power laser bar for 980-nm laser bar at 1105 A (100 μs, 10 Hz) using 29 emitters with 44% FF [5]. FBH reported 1.5 kW peak power and of 58% PCE (at 1 kW) at 25 °C in QCW operation (1.2 ms, 10 Hz) for 940 nm laser bars with 6 mm cavity length and 72% fill factor [6]. As reported by Crump *et al.*, one way to improve power and efficiency is to lower the operating temperature of diode lasers [2]. At low temperature (−50 °C, compared with 25 °C), the slope efficiency was demonstrated to increase by about 10% with a much higher PCE. In the Cryolaser project, a passively cooled 1-cm wide diode laser bar reached an output power of 1.98 kW (2 kA) at a low heatsink temperature $T_{HS} = 203$ K in QCW operation [7], with the PCE of 64% at 1 kW. This is the highest reported power for a single laser bar so far [8]. The laser materials were intentionally optimized for the low-temperature operation to maximize PCE by reducing the aluminum composition of the barrier [9]–[11]. Subsequently, a 4-mm long 940 nm diode laser bar with the efficiency of 70% at an output power of 1 kW operated at 203 K was reported in 2016 [10].

Besides stacking bars for high energy pumping [12], another approach for power scaling is to stack multiple laser structures together on a single substrate during the material epitaxy process by utilizing a tunnel junction structure [13]. In theory, each electron-hole pair of an N-junction epitaxially stacked laser can generate as many as N photons. This means that the internal quantum efficiency of the epitaxially stacked laser is N times larger than that of the corresponding single-junction laser, and obviously, the total power will be proportional to the number of junctions. Several studies have shown that the epitaxial stacking of hetero-structures can provide effective scaling of differential quantum efficiency by the integration of high-efficiency active regions and tunnel junctions [13–16]. The developed laser stacks have the advantage of enhanced power and brightness. Employing this technology, nLight Corp. [17] reported 1.8 kW from a 1-cm-wide and 3-mm-long cavity (with 80% FF) emitting at 88x-nm under 1 kA QCW drive current (200 μs, 14 Hz), at 10 °C.

Recently, we reported QCW operated 940-nm diode laser bars with 1025 W peak power at 25 °C as a result of design optimization and advanced micro-channel-cooled (MCC) package [18]. In this paper, by employing this high-efficiency structure, we present the result of our recent development of epitaxial stacking of two active regions by a tunnel junction for further power scaling. We have achieved a record output power of 1.91 kW for a bar at 1 kA QCW drive current (200 μs, 10 Hz) with 61.1% peak efficiency at room temperature.

The paper is organized as follows. In section 2, the design of a single p-i-n structure and tunnel junction are discussed and the chip simulation results are presented to explore and optimize the device parameters such as the front facet reflectivity and bar fill factor. In section 3, a brief laser fabrication process and a thorough analysis of experimental test results are presented. Then the conclusion and possible future direction are discussed in section 4.

2. Structure Design and Simulation

As shown in Fig. 1(a), the epitaxially stacked double-junction structure consists of two almost identical p-i-n structures connected by a GaAs tunnel junction. The difference between the two p-i-n structures is adjusted by the position of the GaAs TJ. The tunnel junction is 14-nm thick for both n-type and p-type layers and is doped to the levels of $>3 \times 10^{19}$ cm^{-3} with Te in the n-side and $>1 \times 10^{20}$ cm^{-3} in the p-side with C. The tunnel junction position was also optimized for efficiency by balancing the total chip resistance, optical losses of the cladding layers, and the tunnel junction.

The p-i-n structure shown in Fig. 1(b) was optimized, including the thickness, doping, and composition of each layer, as listed in Table 1. The separation between them is large enough to avoid the optical coupling between the two laser structures. This was achieved by ensuring the optical overlap for a 200-nm-thick layer at the middle point of the two p-i-n structures to be less than

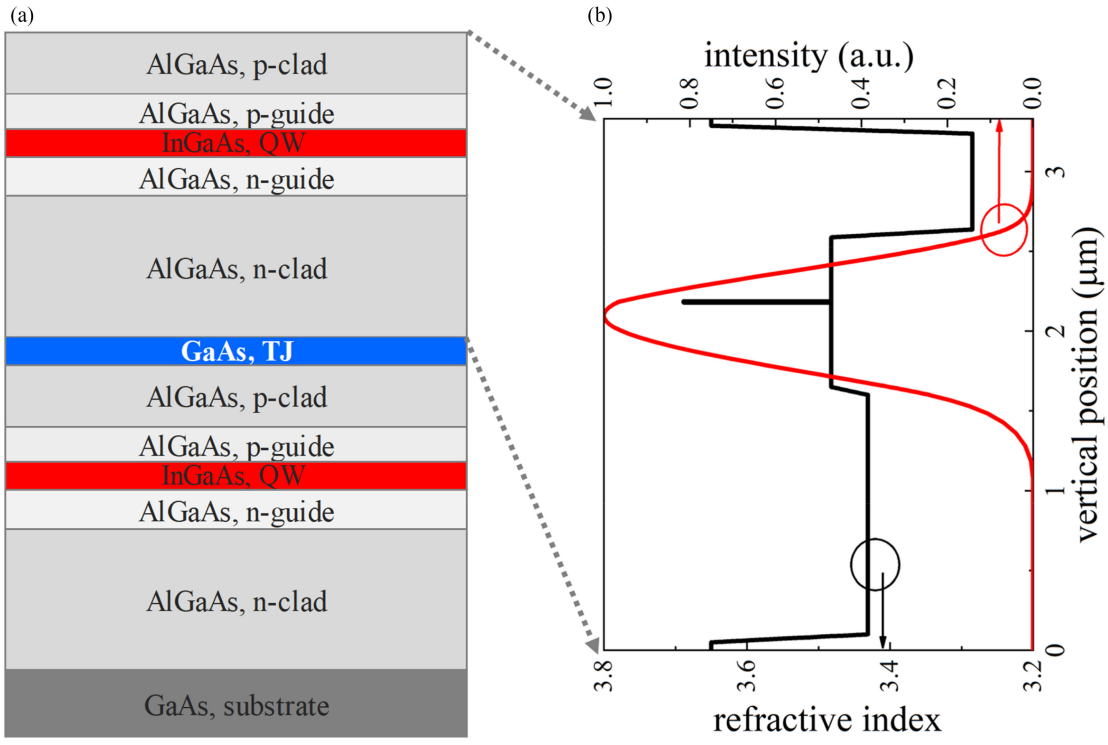

Fig. 1. (a) The epitaxially stacked double-junction structure. (b) Profiles of refractive index and calculated intensity of the fundamental vertical mode of single p- i-n structure.

Table 1
The Single P-I-N Epitaxial Structure

Layer	Composition	Doping (cm^{-3})	Thickness (μm)
p-cap	GaAs	5×10^{19}	0.05
p-cladding	$Al_{0.5}Ga_{0.5}As$	3×10^{18}	0.6
p-waveguide	$Al_{0.25}Ga_{0.7}As$	Undoped	0.4
Active region (QW)	InGaAs	Undoped	0.007
n-waveguide	$Al_{0.25}Ga_{0.7}As$	Undoped	0.53
n-cladding	$Al_{0.3}Ga_{0.7}As$	1×10^{18}	1.5
n-TJ	GaAs	3×10^{19}	0.014
p-TJ	GaAs	1×10^{20}	0.014

5 x 10^{-6}. The vertical design used a compressively strained InGaAs single quantum well (SQW) emitting at 940 nm, embedded in a 0.93 μm thick waveguide with a p-guide thickness of 0.4 μm. The overlap between the fundamental vertical mode and the p-guide was significantly reduced and thus the internal optical loss [2], [19], [24]. A relatively higher Al composition ($Al_{0.5}Ga_{0.5}As$) in the p-clad layer was designed for a high potential barrier to prevent electrons from leaking into the

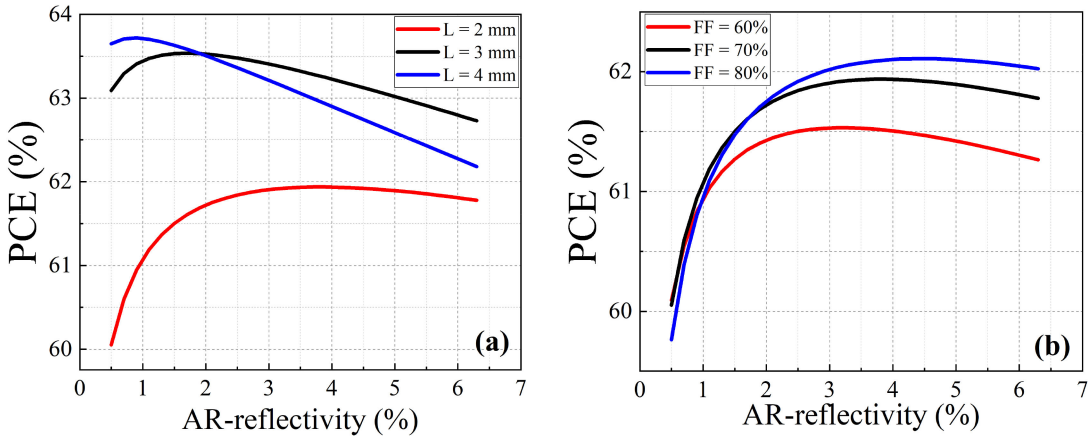

Fig. 2. The dependence of simulated power conversion efficiency (PCE) on the reflectivity of the anti-reflection (AR) coating as well as the cavity length (a) for bar fill factor of 70%, and the bar fill factor (b) for the cavity length of 2 mm.

p-clad layer. However, a lower Al composition ($Al_{0.3}Ga_{0.7}As$) was used in the n-clad layer to reduce the resistance and control the vertical optical mode.

In addition to single emitter efficiency and tunnel junction optimization by the epitaxial design of experiments, bar parameter optimization is also one of the three key components to achieving power scaling. Chip optimization was made using our house-developed laser simulator. The simulator can perform the calculation of internal quantum efficiency for a quantum well structure and its material gain, optical modes in a waveguide, optical loss for a laser structure, temperature distributions for packaged laser modules, as well as L-I-V characteristics for a given package and operation conditions. In the simulation study, the optical output power P_{out} of a laser diode is described by

$$P_{out}(I,t) = \frac{\eta_i(I,t)h\nu}{q}(I - I_{th}(I,t))\frac{\alpha_m}{\alpha_i(I,t)+\alpha_m} \tag{1}$$

where $\eta_i(I,t)$ is the internal quantum efficiency, $I_{th}(I,t)$ is the threshold current, $\alpha_i(I,t)$ is the internal optical loss and α_m is the mirror loss by the facets [20]. To achieve the maximum output power P_{out}, it is necessary to obtain an epitaxial structure with high η_i, low $I_{th,}$ and low α_i. The loss of each layer due to free carrier absorption was calculated using the following classical model

$$\alpha_i = \sum \Gamma_j \left(\sigma_n n_j + \sigma_p p_j\right) \tag{2}$$

where α_i is the internal optical loss, Γ_j is the optical confinement factor in the j_{th} layer, σ_n and σ_p are the free electron and hole absorption cross-sections, n_j and p_j are the carrier concentrations for electrons and holes, respectively [21]. The values of $\sigma_n = 4\times10^{-18}$ cm^{-2} and $\sigma_p = 12\times10^{-18}$ cm^{-2} are used in the simulations [22]. The total internal loss is calculated to be 0.46 cm^{-1}, which confirms the optimization of the vertical p-i-n structure design.

The simulation was based on the following assumptions: 1) chips are mounted p-side-down on MCC heat-sinks; 2) lasers are operated under QCW conditions with a pulse width of 200 μs and repetition rate of 10 Hz; 3) the operation power is 1000 W. Fig. 2 shows the dependence of our simulated power conversion efficiency on the reflectivity of the anti-reflection (AR) coating for the output facet, the cavity length and bar fill factor. In Fig. 2, one can see that there is an optimum AR-reflectivity value to maximize PCE. Besides the AR-reflectivity, both the cavity length and bar fill factor influence efficiency significantly. The cavity length and the bar fill factor affect the thermal resistance and current density of the chips, and thus they impact the chip's joule heating and consequently the power conversion efficiency. As shown in Fig. 2(a) for 70% fill factor, the maximum PCE is calculated to be 63.7% for a 4-mm long cavity, and 62% for a 2-mm long cavity.

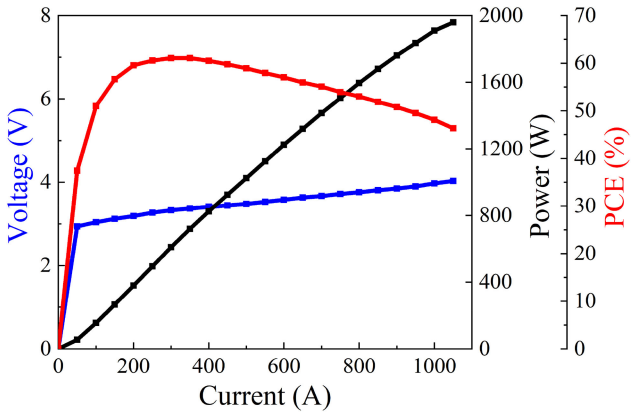

Fig. 3. Power (black), voltage (blue) and PCE (red) versus QCW current at 25 °C.

So, there is a small improvement in achievable PCE with cavity length that makes 2-mm long cavity a reasonable choice on cost grounds. Fig. 2(b) illustrates the impact of the bar fill factor on PCE for a 2-mm long cavity. One can see that the PCE improves from 61% for 60% fill factor to slightly higher than 62% for 80% fill factor. In our design, we choose the bar fill factor to be 70% rather than 80% since there is a marginal increase in the efficiency but a substantial increase in the threshold current. Although the highest PCE of around 63.7% (for 70% fill factor) is calculated for a 4-mm cavity with 1% AR reflectivity, the lowest operation current was calculated for a 2-mm long cavity.

3. Laser Fabrication and Test Results

The epitaxial structure with double laser junctions was grown on n^+ GaAs substrate by metal-organic chemical vapor deposition (MOCVD). Then the wafers were processed using standard photolithography and wet-chemical etching, followed by SiN_x deposition, metallization of Ti/Pt/Au as the p-electrode, substrate thinning, and deposition of AuGeNi/Au as the n-electrode. After cleaving into 1-cm laser bars with 2-mm long cavity and 70% fill factor (37$\times$190 um emitters, optically and electrically isolated by deep trenches), the facets were passivated for high power operation and coated with 3.5% and 96% for the front and back reflectivity, respectively. Then the laser bars were mounted p-side down onto an active micro-channel cooler (MCC) submount with the indium solder, which is much more effective in heat dissipation than conductively cooled package (CCP). Finally, the bars were tested under QCW conditions with a 200 μs pulse width and 10 Hz repetition rate.

Fig. 3 shows the output power, voltage, and power conversion efficiency versus QCW drive current at 25 °C. Below the onset of the thermal rollover, the slope efficiency is 2.23 W/A, which is nearly twice the value of that of the single junction [3]$^-$4 5 6],[8], [18] and it is in line with low internal loss and high carrier injection efficiency. The maximum output power measured at 1000 A is as high as 1.91 kW and it increases to 1.96 kW at 1050 A. The peak PCE of 61.1% at 300 A is comparable to the simulation results. The threshold current is 31 A, corresponding to the threshold current density (J_{th}) of 155 A·cm^{-2}, which is consistent with low internal loss. With increasing current, the slope efficiency remains above 1.88 W/A until 800 A, which is attributed to the fact that carrier leakage in our laser is suppressed well at high currents.

The power-current (P-I) characteristics of 2-mm laser bars at various heatsink temperatures are presented in Fig. 4(a). As the temperature is reduced from 25 °C to 15 °C, the maximum power improves to 1950 W. For T_{HS} at 45 °C, output power reduces to 1765W. Fig. 4(b) shows that the PCE improves slightly for the 15 °C operation. Our voltage data indicate that the turn-on voltage rises marginally with reduced temperature, which is attributed to the broadening of the bandgap and some interface effects caused by contacts or other hetero-barriers [23]. However, the power increase has a higher impact on PCE that reaches 61.3% at 15 °C and drops to 58.8% at 45 °C, which is in agreement with previous studies [6]–[10].

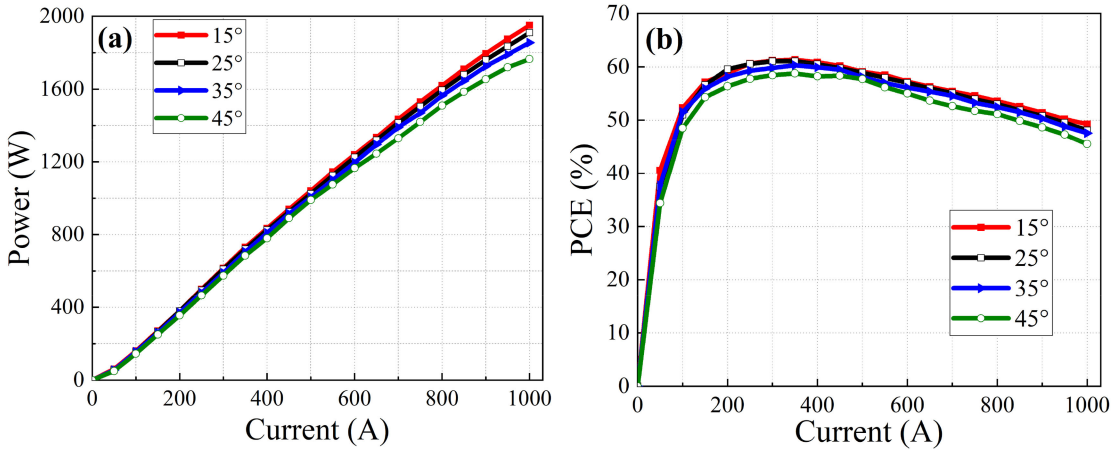

Fig. 4. (a) Power (b) PCE versus QCW current at different heatsink temperatures of 15, 25, 35, 45 °C.

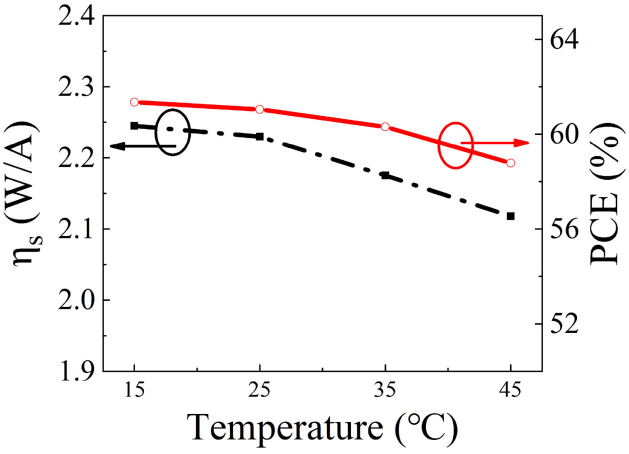

Fig. 5. Slope efficiency η_s and PCE at the current of 350 A against heatsink temperature T_{HS}.

To explain the degradation of power and efficiency with the rise in the T_{HS}, the slope efficiency η_s, extracted from the P-I curves, is plotted against T_{HS} in Fig. 5. The slope efficiency decreases from 2.25 W/A at 15 °C to 2.12 W/A at 45 °C, and the characteristic temperature decreases from 1497 K at 15 °C to 511 K at 45 °C. As the temperature rises, the internal quantum efficiency becomes deteriorated because of the increased carrier leakage and the reduced gain. As a result, the carrier concentration in the active region must be increased to maintain lasing [24] and this will lead to an increased optical loss in the active region. Both the increase in optical loss and the decrease in internal quantum efficiency will result in reduced slope efficiency.

To intuitively understand this, Fig. 5 also illustrates PCE as a function of the heatsink temperature at 350 A in. It can be seen that both the PCE and the slope efficiency follow a very similar trend, which indicates that the decrease of PCE is mainly due to the degraded slope efficiency caused by the decreased internal quantum efficiency and the increased optical loss.

Fig. 6(a) illustrates the spectra of the device measured at 25 °C at different drive currents. The centroid and peak wavelengths are 940.06 nm and 940.76 nm at 1600 W, and the spectral full-width at the half maximum (FWHM) is only about 8 nm indicating a high degree of spectral uniformity among individual emitters. The centroid wavelength increased from 930.24 nm at 100 A near the threshold to 940.06 nm at 800 A, corresponding to an active region temperature rise

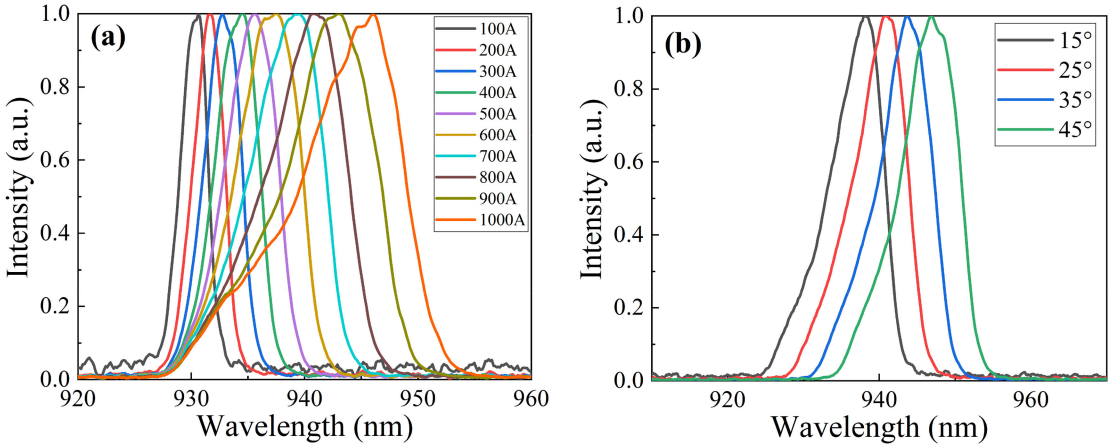

Fig. 6. (a) Emission spectra at 25 °C at different QCW drive currents (b) spectra at 800A at different heatsink temperatures.

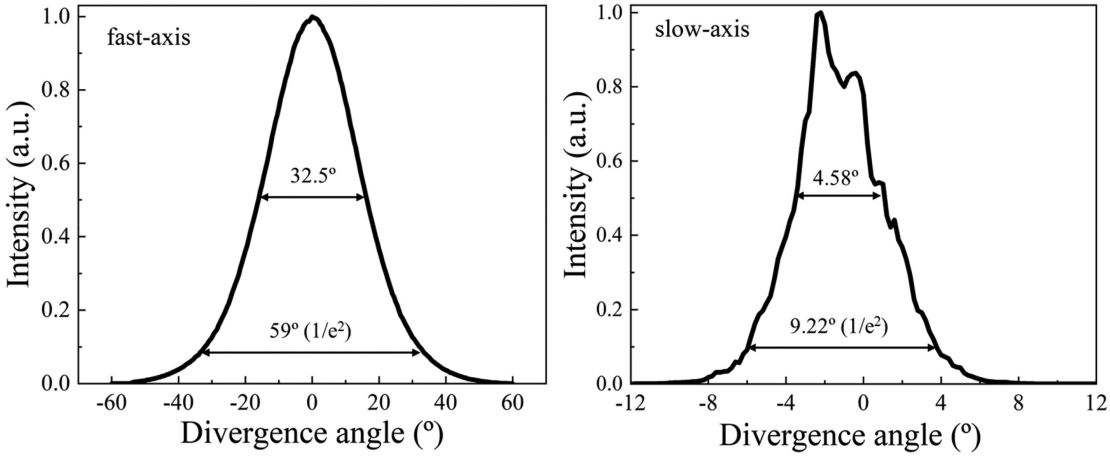

Fig. 7. Far-field intensity measurements of double junction 940nm 2-mm MCC laser bar.

ΔT_{AZ} of 29.8 K, which is calculated by the thermal wavelength drift factor of $\Delta\lambda/\Delta T = 0.326$ nm/K, extrapolated from Fig. 6(b). One can see that the active region temperature increases with current compatible with Fig. 4. Then the higher junction temperature leads to reduced internal quantum efficiency and higher internal loss. Hence, the optical power is gradually saturated.

Besides, Fig. 6(a) shows that the left-hand tail of the spectra expands rapidly, especially at the currents of 0.9 kA and 1 kA. This might be due to the excessive hot carriers occupying the higher energy levels, which leads to the broadening of the Fermi distribution. The carriers in the high-energy states have much lower gain and generate more heat. This would result in a decrease in differential quantum efficiency and further acceleration of power saturation, which is consistent with the P-I curve in Fig. 3. Another possible reason may be that the temperature of lower active region is slightly high than the upper active region caused by further distance from the heatsink, which will aggravate the broadening of the spectrum.

Fig. 7 shows that the far-field divergence angles at FWHM along the fast and slow axis at 800 W are 32.5° and 4.6°, respectively. These results are suitable for use in the efficient pumping of Yb-doped YAG solid-state lasers.

4. Conclusion

We have developed a high-power laser bar by employing a double-junction epitaxial structure. The optimum cavity length (2 mm), AR reflectivity (3.5%) and fill factor (70%) were explored and selected based on the modeling results of our house-developed simulation software. Based on the high-efficiency p-i-n structure and a low resistance single tunnel junction, a record peak power of 1.91 kW was obtained at 1 kA drive current (QCW, 200 μs, 10 Hz) at 25 °C. The maximum power conversion efficiency of 61.1% was achieved at 300 A. Further improvement in the power and efficiency can be realized by employing a longer cavity and a slightly larger bar fill factor as suggested by our theoretical calculations. Another possible direction for further power and brightness scaling from a single bar can be to include more tunnel junctions that would require strain compensation with thicker epitaxial growth and thermal management.

References

[1] E. Zucker *et al.*, "Advancements in laser diode chip and packaging technologies for application in kW-class fiber laser pumping," in *Proc. SPIE*, vol. 8965, no. 896507, 2014, pp. 1–14.

[2] P. Crump *et al.*, "Efficient high-power laser diodes," *IEEE J. Sel. Topics Quantum Electron.*, vol. 19, no. 4, pp. 1–11, Jul./Aug. 2013.

[3] P. Crump *et al.*, "Cryogenic ultra-high-power infrared diode laser bars," in *Proc. SPIE*, vol. 9002, no. 90021I, pp. 1–11, 2014.

[4] H. Li *et al.*, "Reliable high-efficiency high brightness laser diode bars at 940 nm," *Opt. Laser Technol.*, vol. 36, pp. 327–329, 2004.

[5] D. Schröder *et al.*, "Increased power of broad area lasers (808 nm /980 nm) and applicability to 10 mm-bars with up to 1000 watt QCW," in *Proc. SPIE*, vol. 6456, no. 64560N, pp. 1–10, 2007.

[6] P. Crump *et al.*, "Cryolaser: Innovative cryogenic diode laser bars optimized for emerging ultra-high power laser applications," in *Proc. CLEO Conf. Lasers Electro Opt.*, no. JW1J.2, 2013, pp. 1–2.

[7] C. Frevert *et al.*, "Low-temperature optimized 940 nm diode laser bars with 1.98 kW peak power at 203 K," in *Proc. CLEO Conf. Lasers Electro Opt.*, no. SM3F.8, 2013, pp. 1–2.

[8] P. Crump and G. Tränkle, "A brief history of Kilowatt-class diode-laser bars," in *Proc. SPIE*, vol. 11301, no. 113011D, 2020, pp. 1–9.

[9] C. Frevert *et al.*, "Study of waveguide designs for high power 9xx-nm diode lasers operating at 200 K," in *Proc. SPIE*, vol. 8965, no. 89650O, 2014, pp. 1–11.

[10] C. Frevert *et al.*, "940 nm QCW diode laser bars with 70% efficiency at 1 kW output power at 203 K: Analysis of remaining limits and path to higher efficiency and power at 200 k and 300 K," in *Proc. SPIE*, vol. 9733, no. 97330L, 2016, pp. 1–13.

[11] C. Frevert *et al.*, "The impact of low Al-content waveguides on power and efficiency of 9xx nm diode lasers between 200 and 300k," *Semi. Sci. Technol.*, vol. 31, no. 025003, pp. 1–12, 2016.

[12] N. Kageyama *et al.*, "Development of high-power quasi-CW laser bar stacks with enhanced assembly structure," *IEEE Photon. Tech. Lett.*, vol. 28, no. 9, pp. 983–985, May 2016.

[13] J. Ch. Garcia *et al.*, "Epitaxially stacked lasers with esaki junctions: A bipolar cascade laser," *Appl. Phy. Lett.*, vol. 71, no. 29, pp. 3752–3754, 1997.

[14] A. Lyakh and P. Zory, "Gallium-Arsenide-based bipolar cascade lasers with deep quantum-well tunnel junctions," *IEEE Photon. Technol. Lett.*, vol. 18, no. 24, pp. 2656–2658, Dec. 2006.

[15] E. I. Davydova *et al.*, "High-power laser diodes based on triple integrated ingaas/algaas/gaas structures emitting at 0.9 um," *Quantum Electron.*, vol. 39, no. 8, pp. 723–726, 2009.

[16] A. A. Marmalyuk *et al.*, "Laser diodes with several emitting regions (λ = 800-1000 nm) on the basis of epitaxially integrated heterostructures," *Semiconductors*, vol. 45, no. 4, pp. 519–525, 2011.

[17] M. Kanskar *et al.*, "High power and high efficiency 1.8-kW pulsed diode laser bar," *J. Photon. for Energy*, vol. 7, no. 1, pp. 1–8, 2017, Art. no. 016003.

[18] Y. Zhao *et al.*, "Research on 940nm kilowatt high efficiency quasi- continuous diode laser bars," in *Proc. SPIE*, vol. 11170, no. 1117040, 2019, pp. 1–6.

[19] X. Wang *et al.*, "Root-cause analysis of peak power saturation in pulse-pumped 1100nm broad area single emitter diode lasers," *IEEE J. Quantum Electron.*, vol. 46, no. 5, pp. 658–665, May 2010.

[20] P. W. Epperlein, *Semiconductor Laser Engineering, Reliability and Diagnostics: A Practical Approach to High Power and Single Mode Devices*. West Sussex, U.K.: Wiley, 2013.

[21] N. A. Pikhtin *et al.*, "Internal optical loss in semiconductor lasers," *Semiconductors*, vol. 38, no. 3, pp. 360–367, 2004.

[22] M. Peters *et al.*, "High power, high efficiency laser diodes at JDSU," in *Proc. SPIE*, vol. 6456, no. 64560G, 2007, pp. 1–11.

[23] P. O. Leisher, W. Dong, M. P. Grimshaw, M. J. DeFranza, M. A. Dubinskii, and S. G. Patterson, "Mitigation of voltage defect for high-efficiency InP diode lasers operating at cryogenic temperatures," *IEEE Photon. Technol. Lett.*, vol. 22, no. 24, pp. 1829–1831, Dec. 2010.

[24] T. Kaul *et al.*, "Impact of carrier nonpinning effect on thermal power saturation in gaas-based high power diode lasers," *IEEE J. Sel. Topics Quantum Electron.*, vol. 25, no. 6, pp. 1–10, Nov./Dec. 2019.